高数值孔径系统多重初级像差对高斯光束的影响

李红福[1,2]，解慧明[3]，张琛[1]，王凯歌[1]，王爽[1]，贺庆丽[2]，白晋涛[1]

（1 西北大学 光子学与光子技术研究所 省部共建光电技术与功能材料国家重点实验室培育基地，西安 710069）

（2 西北大学 物理学院，西安 710069）

（3 西安市教育科学研究所，西安 710003）

摘　要：为了揭示高数值孔径光学系统在多重初级像差共同作用时受到的影响，基于衍射理论，研究了多重初级像差，特别是彗差、象散和球差对汇聚高斯光束的影响效果．通过数值模拟计算，获得了在彗差、象散和球差共同作用下，汇聚高斯光束在焦平面处光斑的光强分布，发现多重像差对聚焦光斑的影响并非各单像差影响效果的简单叠加．通过对高数值孔径光学系统激光焦斑的实际测量，发现其光强分布特点与数值模拟结果具有高度的一致性．研究结果对于评估与分析实际的光学系统具有一定的指导意义．

关键词：多重初级像差；高数值孔径；衍射理论；高斯光束；数值模拟

中图分类号：O43　　文献标识码：A　　　　　　文章编号：1004-4213(2015)09-0912001-7

Studying the Combined Effects of Primary Aberrations on Gaussian Beam in High NA Focusing System

LI Hong-fu[1,2], XIE Hui-ming[3], ZHANG Chen[1], WANG Kai-ge[1],
WANG Shuang[1], HE Qing-li[2], BAI Jin-tao[1]

(1 *Institute of Photonics & Photo-Technology，Northwest University，Xi'an 710069，China*)

(2 *Physics Department，Northwest University，Xi'an 710069，China*)

(3 *Xi'an Education Scientific Research Institute，Xi'an 710003，China*)

Abstract：For purpose of revealing the negative impacts of multiple primary aberrations in high numerical aperture optical system，the combined influence of the primary aberrations，especially coma，astigmatism and spherical aberration，on focusing Gaussian beam in high numerical aperture system was carried out based on diffraction theory. The intensity distribution of the Gaussian beam focal spot suffering multiple influence of coma，astigmatism and spherical aberration were acquired by numerical simulation. The results show that the impact of multiple abration was not only superimposed of single aberration. In addition，a high consistency was found between the simulation results and the laser spots captured on the focal plane of a self-made high numerical aperture system，which indicated the reliability and reasonableness of the numerical simulation. The results present the optical distribution properties of Gaussian beam receiving multiple primary aberration effects，which will be helpful for evaluating and analyzing the practical optical focusing system.

Key words：Multiple primary aberration；High numerical aperture；Diffraction theory；Gaussian beam；Numerical simulation

OCIS Codes：050.1970；080.1010；120.4820

http：//www.photon.ac.cn

0　Introduction

The Gaussian beam has been widely applied in lithography[1] optical fabrication[2-4], atoms capture[5-7], super resolution technology[8] far-field microscopy[9-10] and imaging[11-12], with high Numerical Aperture(NA) objective collection. Generally, in the high NA optical system, the beam is unavoidably impacted by optical aberration which results in distortion of the focal sphere. The individual effects of primary aberrations on spatio-temporal characters of the focused Gaussian beam have been revealed by many researchers[13-15]. The image formation in high NA focusing systems with Seidel aberrations have been theoretically studied by R. Kant[16-17]. R. K. Singh et al. analyzed the primary aberrations effect in focusing Laguerre-Gaussian beam of high NA system with different topological charge[18-21]. S. H. Deng′s group investigated the depletion patterns which are affected by individual primary aberrations[22-23].

However, the multiple primary aberration is usually borne at the same time in a realistic optical system. While, its induced influence effect and mechanism on the whole optical system have not yet been completely and accurately disclosed. In practical system, e. g., the stimulated emission depletion microscopy, the Gaussian beam is modulated to a kind of circular shaped-beam by phase plate, it is also influenced by multiple primary aberrations and the situation is more complicated. With the combined aberration effects, the focal spot is twisted into different appearances, and has different intensity distribution and size.

In this paper, we will make a simulation study on the multiple effects such as coma, astigmatism and spherical aberration on focusing Gaussian laser beam with high NA lens. The laser pattern is calculated with different aberration coefficients. The characters of the laser spots in simulation are quantitative revealed and analyzed, and the experimental data are highly consistent with the simulation results. This work will be helpful for assembling and analyzing the Gaussian laser system in realistic situations.

1　Theory

Fig. 1 is the theoretical model for investigating the influence of multiple aberration effects on Gaussian beam. A right-handed circular polarized beam is employed with an objective (NA＝1.4) in the system.

The electric field vector E at a point p (r_p, φ_p, z_p) in cylindrical coordinates with the origin located at focal point can be expressed by generalized Debye integral as Eq. (1)[17,24].
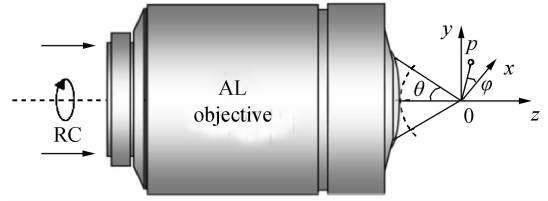

Fig. 1　Theoretical model for simulation.
(AL, Aplanatic Lens)

$$\boldsymbol{E}(r_p,\varphi_p,z_p) = \mathrm{i}\frac{fl_0}{\lambda}\int\int_{\Omega}\sqrt{\cos\theta}\sin(\theta)\cdot E_0\cdot \boldsymbol{V}(\theta)\cdot$$

$$A_1(\theta,\varphi)\times\begin{bmatrix}\boldsymbol{P}_x\\\boldsymbol{P}_y\\\boldsymbol{P}_z\end{bmatrix}\exp\{ikn[z_p\cos\theta+r_p\sin\theta\cdot$$

$$\cos(\varphi-\varphi_p)]\}\mathrm{d}\theta\mathrm{d}\varphi \tag{1}$$

where, f represents the focal length of the lens and l_0 is the amplitude factor in the image space, λ stands for the wavelength of incident light.

The Gaussian light at the pupil of objective is expressed as $E_0 = I_0\exp(-\gamma^2\sin^2\theta/\sin^2\theta_{max})$. I_0 is the light intensity and assumed to 1 in the calculation. γ is the truncation parameter that describes the beam inside the physical aperture; it is expressed as $\gamma = a/\omega$ (a is aperture radius and ω is the beam size at waist). θ represents the angle between light direction and optic axis, θ_{max} is the maximal semi-aperture angle of objective lens ($\theta_{max} = 67°$) and φ stands for the azimuthal coordinate at the input plane. $\boldsymbol{V}(\theta,\varphi)$ is the conversion matrix of the polarization from the object field to the image field.

$$\boldsymbol{V}(\theta,\varphi)=\begin{bmatrix}1+(\cos\theta-1)\cos^2\varphi & (\cos\theta-1)\cos\varphi\sin\varphi & -\sin\theta\cos\varphi\\(\cos\theta-1)\cos\varphi\sin\varphi & 1+(\cos\theta-1)\sin^2\varphi & -\sin\theta\sin\varphi\\\sin\theta\cos\varphi & \sin\theta\sin\varphi & \cos\theta\end{bmatrix} \tag{2}$$

$A_1(\theta,\varphi)$ is the aberration wavefront function. Here, it is given as the Eq. (3).

$$A_1(\theta,\varphi)=\exp[A_c(\theta,\varphi)+A_a(\theta,\varphi)+A_s(\theta,\varphi)] \tag{3}$$

where, $A_c(\theta,\varphi)$, $A_a(\theta,\varphi)$ and $A_s(\theta,\varphi)$ represent wavefront aberration functions of coma, astigmatism and spherical aberration, respectively. They can be expressed as following:

$$A_c(\theta,\varphi)=ika_c\left(\frac{\sin\theta}{\sin\theta_{max}}\right)^3\cos\varphi \tag{4}$$

$$A_a(\theta,\varphi)=ika_a\left(\frac{\sin\theta}{\sin\theta_{max}}\right)^2\cos^2\varphi \tag{5}$$

$$A_s(\theta, \varphi) = ika_s \left(\frac{\sin \theta}{\sin \theta_{max}} \right)^4 \qquad (6)$$

where, a_c, a_a and a_s are the aberration coefficient of coma, astigmatism and spherical aberration sequentially.

$[\boldsymbol{p}_x, \boldsymbol{p}_y, \boldsymbol{p}_z]$ is defined as the matrix unit of the polarization of incident light. $k = 2\pi n/\lambda$, which means the wave number, n is the refractive index of the focal space medium ($n = 1.52$). For focal plane, z_p equals to 0.

2　Results and discussion

2.1　Effect of coma and astigmatism

Generally, the coma and astigmatism are the most negative influence factors to the laser focus[16]. Thus, the numerical study of the influences of the comatic aberration and astigmatism are prioritized studied in the following. We use Matlab in the simulation.

Fig. 2 is the intensity distributions calculated with different parameters of a_c and a_a values. a_c and a_a refer to the deviation of the wavefront to the Gaussian reference sphere. During the simulation, the value of a_c and a_a are chosen from 0 to 0.6λ and 0 to 0.35λ respectively owing to the aberration tolerance; the parameter of a_c changes 0.12λ for each step, and a_a changes 0.07λ for each step. It is obvious that with the combined effects of coma and astigmatism, the distribution of light intensity is non-uniform in the focal spot. The variation rule of the patterns is also complex than that influenced by single aberration. For instance, when $a_c = 0.12\lambda$, $a_a = 0.28\lambda$, the laser spot is water-drop shaped.
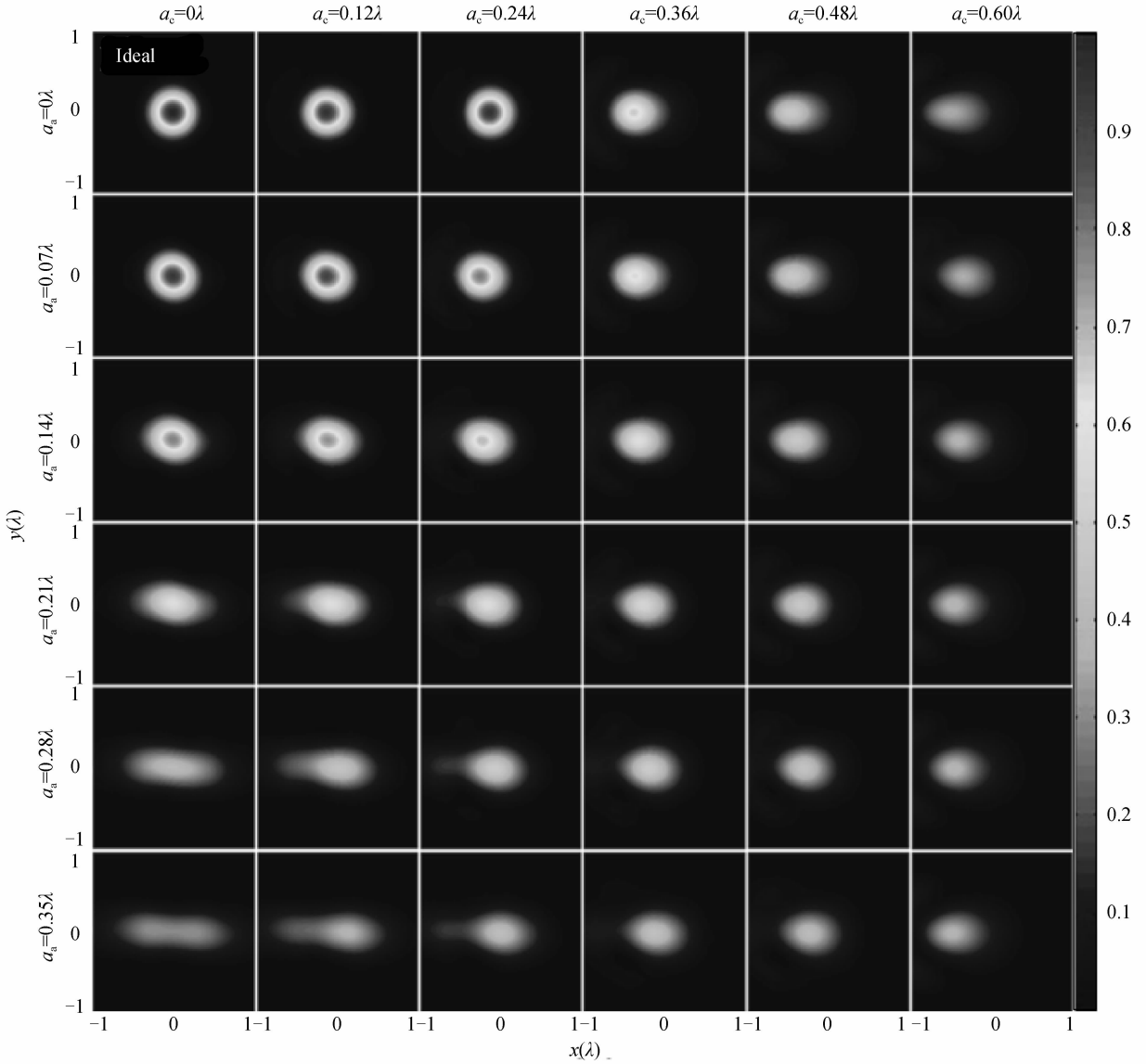

Fig. 2　Simulation results of focal spot with different coma and astigmatism coefficient

Fig. 3 reveals the size variation of laser spot at FWHM when the constant a_c and a_a are in the range: $0 \leqslant a_c \leqslant 0.6\lambda$, $0 \leqslant a_c \leqslant 0.35\lambda$. In the case of $a_c = a_a = 0$, the pattern is ideal (see Fig. 2), and the Full Width at Half Maximum (FWHM) D equals to 0.375λ. Since the patterns are irregular, the size of pattern is

described in two directions. D_l stands for the length in x direction while D_m in y direction. When $a_c=0$, $a_a=0.35\lambda$, $D_l=1.14\lambda$, $D_m=0.5\lambda$; $a_c=0.6$, $a_a=0\lambda$, $D_l=0.65\lambda$, $D_m=0.48\lambda$; $a_c=0.6\lambda$, $a_a=0.35\lambda$, $D_l=0.54\lambda$, $D_m=0.5\lambda$.
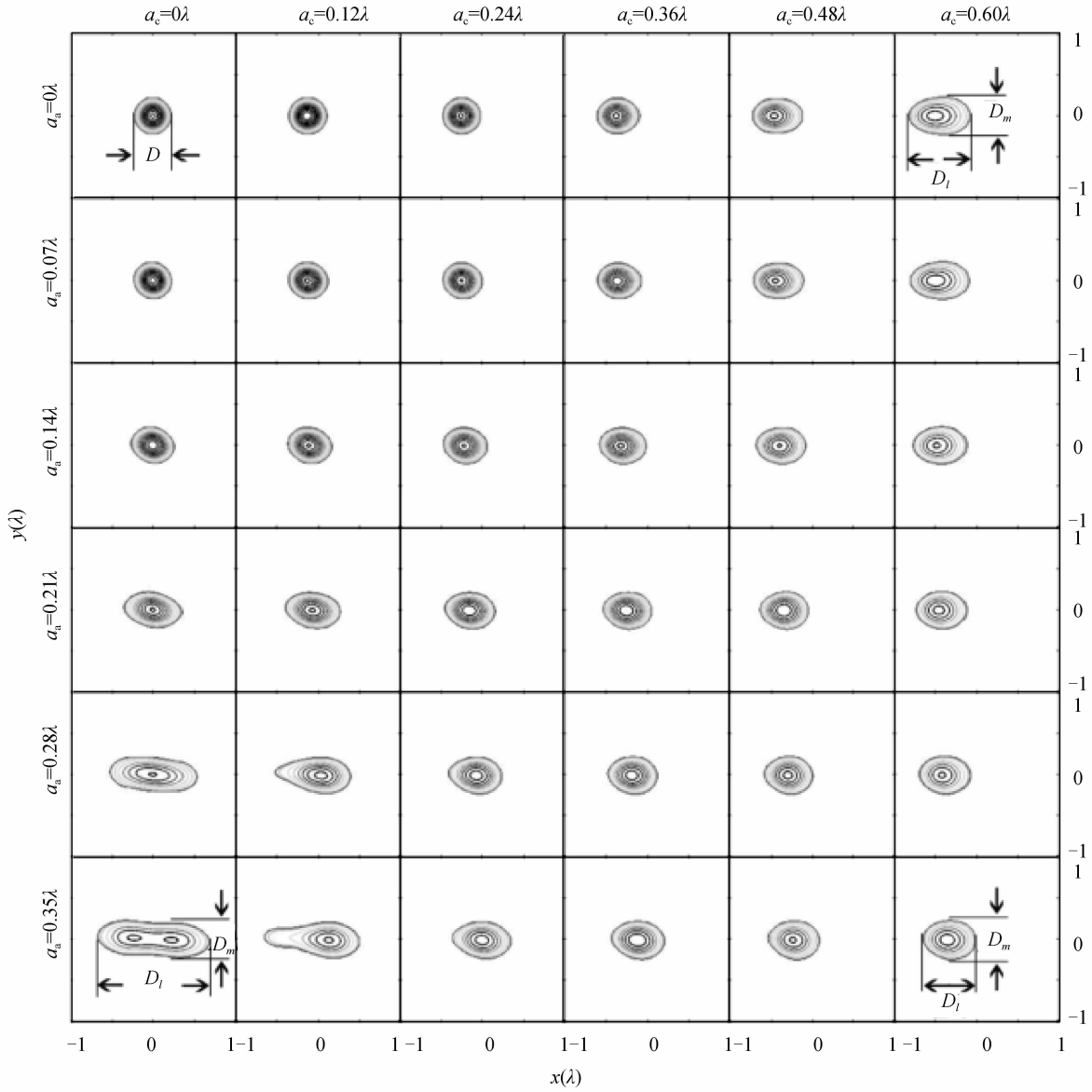

Fig. 3　Isophotes of the focal spot at FWHM corresponding to Fig. 2

The irregular transformation of laser focus on lateral direction is caused by the coma and astigmatism, the former induces asymmetry and the latter leads the laser spot stretching.

Fig. 4(a) illustrates the variation of the maximum normalized intensity of laser patterns in different a_c and a_a. It can be seen clearly, under the same a_c value (equals to 0.23), the maximum intensities decrease quickly when the $a_a \leqslant 0.21\lambda$, while the intensity is enhanced in the situations of $a_a \geqslant 0.28\lambda$, however, it starts to fall when $a_c \geqslant 0.36\lambda$. In general, the maximum value of normalized intensity is reduced with the combined influence of aberrations, i. e., the maximum normalized intensity changes from 1 to 0.3.

Fig. 4(b) displays the change of the focal spot size

of Fig. 3. In the case of $a_a=0\lambda$, 0.07λ and 0.14λ, the focal spots become bigger with the increasing of a_c.
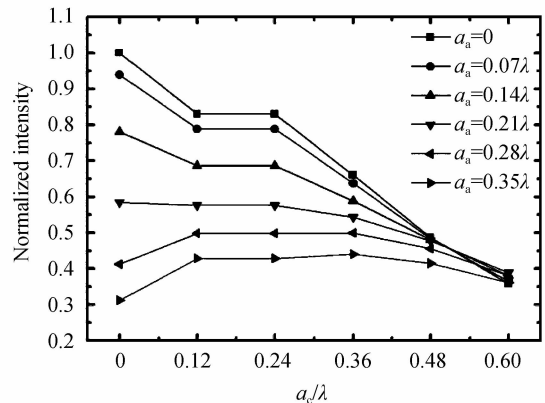
(a) The maximum intensity of the pattern
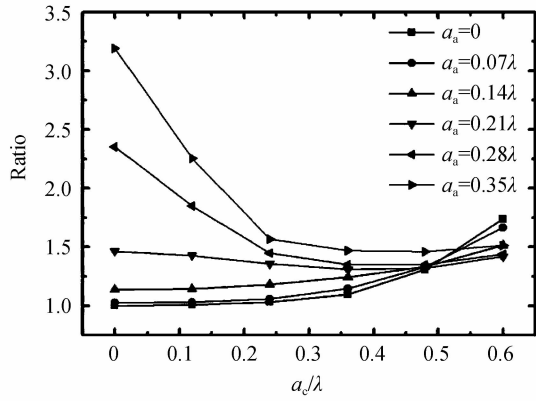
(b) The focal spot dimension at FWHM

Fig. 4　Focal spot pattern variation with different a_c and a_a
When $a_c = 0.6\lambda$, the area of focal spots are 1.74, 1.66 and 1.51 times larger than the ideal pattern. When $a_a = 0.21\lambda$, a_c changes from 0 to 0.6λ, the focal spot is around 1.4 times comparing to the ideal one. In the

situation of $a_a = 0.28\lambda$ and 0.35λ, the area of laser spot decreases when a_c changes from 0 to 0.6λ, the area ratios to the ideal pattern are reduced from 2.39 to 1.44 and 3.19 to 1.51, respectively.

2.2　Effect of coma, astigmatism and spherical aberration

Generally, the spherical aberration contributes to the axial shifting of focus. The spherical aberration usually caused by the immersion oil, the samples or its mounting medium. In the following simulations, the comatic and astigmatism coefficients are assumed to constants ($a_c = 0.12\lambda$, $a_a = 0.07\lambda$). In view of the aberration tolerance condition of focusing system, the coefficient of spherical aberration increases with amount of 0.16λ for each step.

Fig. 5 shows the focus intensity distribution on XZ plane. When $a_c = 0.12\lambda$, $a_a = 0.07\lambda$ and a_s changes from 0.16λ to 0.96λ.
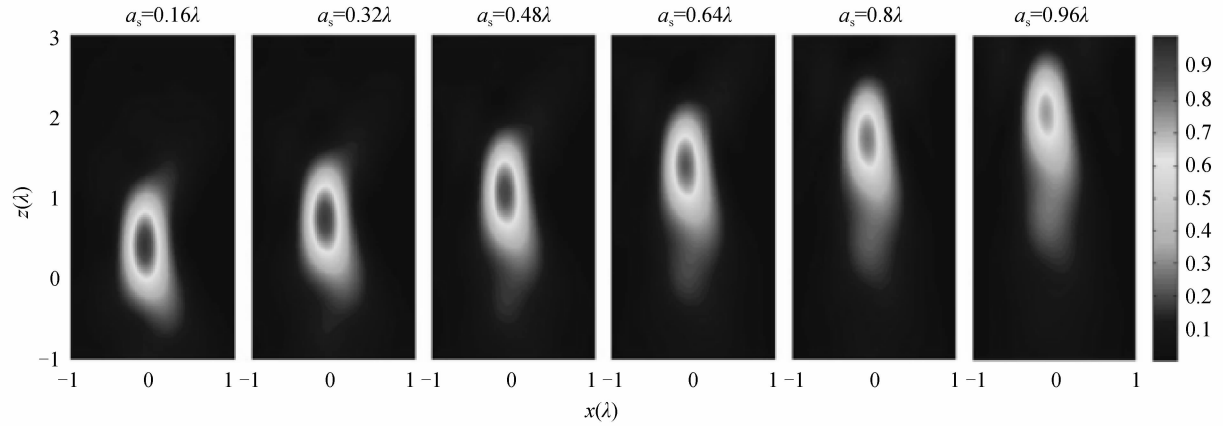

Fig. 5　Axial intensity distribution of laser spots tolerating multiple primary aberrations, $a_c = 0.12\lambda$, $a_a = 0.07\lambda$ and a_s changing from 0.16λ to 0.96λ

Fig. 6 reveals the shift of the best focus position with the enhancing spherical aberration effect. The best focus position moves from 0.4λ to 2.05λ in axial direction when the a_s increases from 0 to 0.96λ.
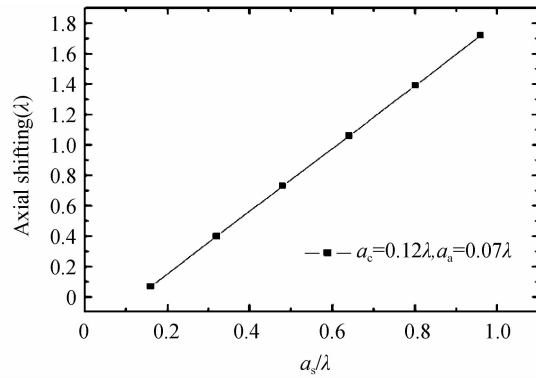

Fig. 6　Best focus position shifting

Fig. 7 presents the laser spot at the best focus position in the case of Fig. 5. It is found that the focal spot does not change much when a_s is increasing, as well as the size of laser spot at FWHM. The maximum intensity of laser spot decreases as the spherical aberration effect strengthening.

Fig. 8 shows the detailed information of laser intensity and the dimension of laser spot at FWHM in Fig. 7. From the Fig. 8 (a), it can be noticed that the maximum normalized intensity of the laser pattern reduced from 0.95 to 0.74 when the spherical aberration increases. The Fig. 8 (b) shows that with the combined effect of primary aberration, the change of the area at FWHM is little (about 1.002 to 1.013 times bigger than that in ideal condition).
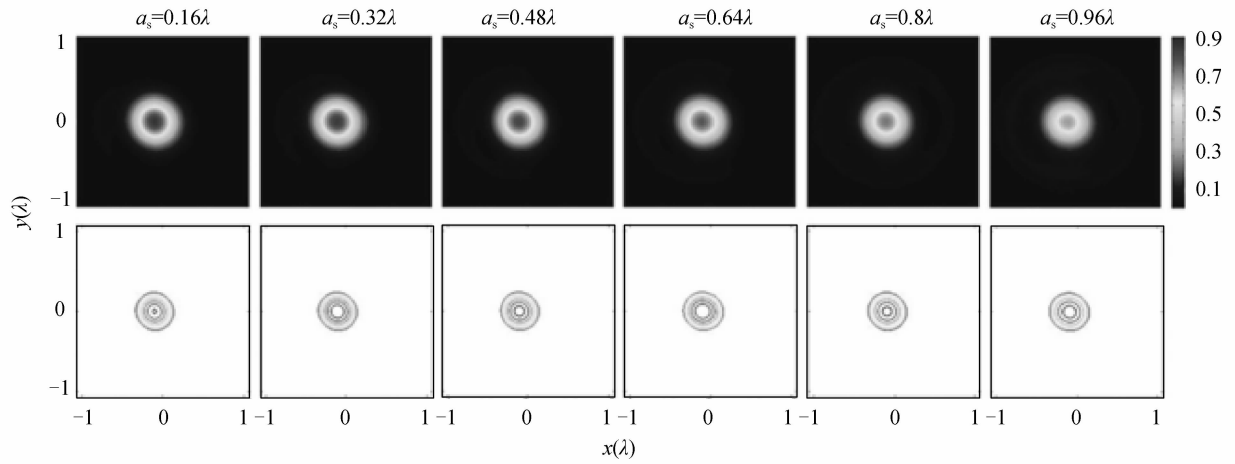
Fig. 7　Laser spots and corresponding laser spot isophotes at FWHM on the best focal plane
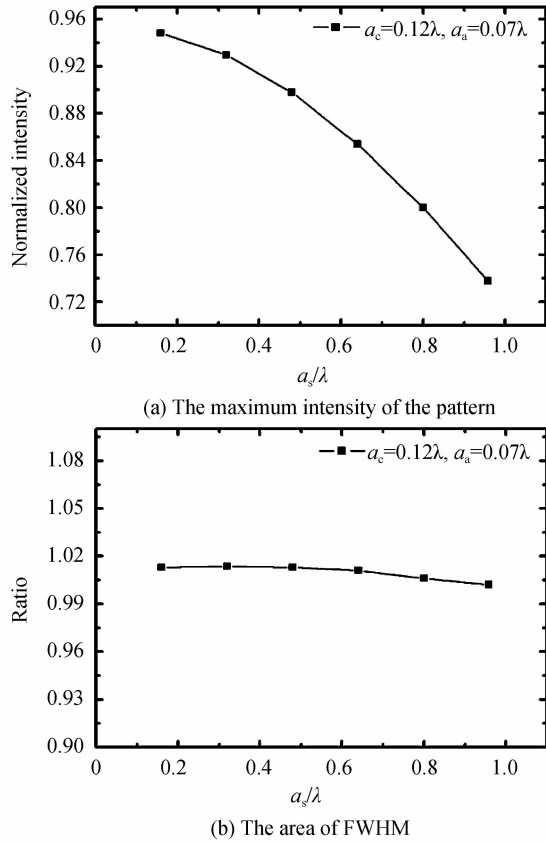

(a) The maximum intensity of the pattern

(b) The area of FWHM

Fig. 8　Variation of the laser pattern with increasing a_s

3　Experiment

With the assist of a home-made CW-laser-direct writing system with high NA objective lens, the impact of optical aberrations on laser spot is experimentally measured. The practical setup is schematic diagrammed as Fig. 9. A linear polarized Gaussian laser beam become circular polarized after passing through a $1/4\lambda$ WP (wave plate), and finally focused by a high NA (×100, NA＝0.9, ZEIZZ) objective. The focal spot image is captured by a CCD camera after the beam reflected by a silver-coated flat mirror.
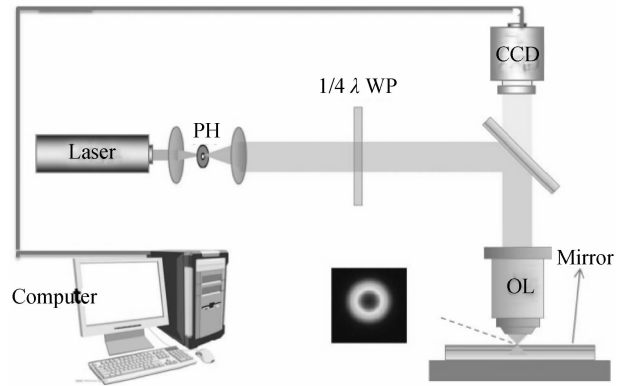

Fig. 9　Schematic diagram of experimental setup

It is well known that the coma effect will emerge out when there forms a slant angle between the axis of objective and incident light beam; the astigmatism effect appears when the objective axis is deviated from the light beam axis. Therefore, through the modulation of the relative position of objective lens corresponding to the incident light beam, different aberrations will be induced to the focal spot.

Fig. 10 shows the laser focal spots suffering primary aberrations. Fig. 10(a) and 10(b) are obtained by slightly adjusting the objective to form tiny angles with the beam axis. The focal spot in Fig. 10 (a) is comet shaped, which is similar to the simulation result in the first row of forth column (Fig. 2). When the angle between the objective and the main light axis become bigger, Fig. 10 (b) is obtained. It looks like the spot of the first row of fifth column in Fig. 2. It is also comet shaped, but has a longer tail on the right. When the angle between the objective and the main light axis become bigger, Fig. 10 (d) is obtained. It is a speckle in comet shape, the intensity on left is higher than the right. It also can be found the corresponding pattern in the simulation results as shown in the Fig. 2, the first row of sixth column.

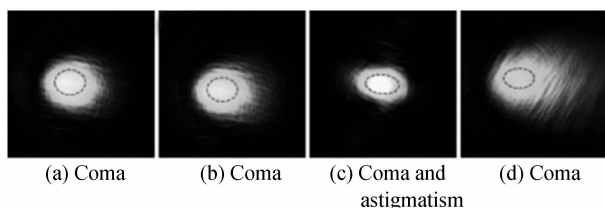(a) Coma   (b) Coma   (c) Coma and   (d) Coma
astigmatism

Fig. 10   Laser experimental focal spots with different primary aberration

While the lateral position of the objective changed, the effect of astigmatism is introduced into the system. The Fig. 10（c）is the focal spot captured when the system is impacted by the aberration of coma and astigmatism. It can be found that the focal spot of the Fig. 10（c）is pear shape. The shape is quite same as the focal spot as shown in the Fig. 2 as the fourth row of third column.

4   Conclusion

The intensity distribution of the laser in high NA focusing system is complicated while suffering combined influence of coma, astigmatism and spherical aberration, the final features are seriously determined by the factors, i. e. a_c, a_a and a_s together.

Generally, the maximum intensity of focal spots decreases with the increasing of a_c and a_a. The area ratio of focal spot at FWHM is increased in the case of $a_a < 0.21\lambda$, while, it will be declined as $a_a > 0.21\lambda$. When the spherical aberration is combined with coma and astigmatism, the best focal plane will shift in axial direction. The maximum intensity is reduced, and the focal spot size at FWHM is barely changed with the growing of a_s.

In addition, it is found a high degree of similarity between the simulation results and experimental laser spots captured by CCD camera. The results are helpful for analyzing the aberration of focal pattern in realistic situations and guiding the setting up practical optical system.

References

[1] JUODKAZIS S, MIZEIKIS V, SEET K K, et al. Two-photon lithography of nanorods in SU-8 photoresist [J]. Nanotechnology, 2005, 16(6): 846-849.

[2] SULLIVAN A C, GRABOWSKI M W, MCLEOD R R. Three-dimensional direct-write lithography into photopolymer [J]. Applied Optics, 2007, 46(3): 295-301.

[3] HOOGH A D, HOMMERSOM B, KOENDERINK A F. Wavelength-selective addressing of visible and near-infrared plasmon resonances for SU8 nanolithography [J]. Optics Express, 2011, 19(12): 11405-11414.

[4] JEON H, SCHMIDT R, BARTON J E, et al. Chemical patterning of ultrathin polymer films by direct-write multiphoton lithography [J]. Journal of the American Chemical Society, 2011, 133(16): 6138-6141.

[5] ASHKIN A. Optical trapping and manipulation of neutral particles using lasers [J]. Proceedings of the National Academy of Sciences, 1997, 94(10): 4853-4860.

[6] SHIMIZU F, SHIMIZU K, TAKUMA H. Four-beam laser trap of neutral atoms[J]. Optics Letters, 1991, 16(5): 339-341.

[7] PINKSE P W H, FISCHER T, MAUNZ P, et al. Trapping an atom with single photons[J]. Nature, 2000, 404: 365-368.

[8] WANG Wei. Super resolution technology of Gaussian beam under high humerical aperture[J]. Acta Photonica Sinica, 2013, 42(4): 441-446.

[9] HELL S W. Far-field optical nanoscopy[J]. Science, 2007, 316(5828): 1153-1158.

[10] HEIN B, WILLIG K I, HELL S W. Stimulated emission depletion (STED) nanoscopy of a fluorescent protein-labeled organelle inside a living cell[J]. Proceedings of the National Academy of Sciences, 2008, 105(38): 14271-14276.

[11] SCHMIDT R, WURM C A, PUNGE A, et al. Mitochondrial cristae revealed with focused light[J]. Nano Letters, 2009, 9(6): 2508-2510.

[12] REUSS M, ENGELHARDT J, HELL S W. Birefringent device converts a standard scanning microscope into a STED microscope that also maps molecular orientation[J]. Optics Express, 2010, 18(2): 1049-1058.

[13] SHI Guang-yuan, YANG Xiao-ping, LIANG Yan-mei. Gaussian beam shaping based on aspheric cylindrical lens[J]. Acta Photonica Sinica, 2014, 43(S1): 0122001.

[14] WANG Shan-shan, DENG Xiao-jiu, LIU Cai-xia, et al. Propagation characteristics of truncated nonparaxial scalar Gaussian beams[J]. Acta Photonica Sinica, 2014, 43(4): 0426003.

[15] ZHOU Ye-peng, REN Hong-liang, WANG Juan, et al. Comparative analysis of the trapping force using Laguerre-Gaussian beam and Gaussian beam [J]. Acta Photonica Sinica, 2013, 42(11): 1300-1304.

[16] KANT R. An analytical solution of vector diffraction for focusing optical systems [J]. Journal of Modern Optics, 1993, 40(2): 337-347.

[17] KANT R. An analytical solution of vector diffraction for focusing optical systems with seidel aberrations: I. Spherical aberration, curvature of field, and distortion[J]. Journal of Modern Optics, 1993, 40(11): 2293-2310.

[18] SINGH R K, SENTHILKUMARAN P, SINGH K. Effect of primary spherical aberration on high-numerical aperture focusing of a Laguerre-Gaussian beam[J]. Journal of the Optical Society of America A, 2008, 25(6): 1307-1318.

[19] SINGH R K, SENTHILKUMARAN P, SINGH K. Focusing of a vortex carrying beam with Gaussian background by an apertured system in presence of coma [J]. Optics Communications, 2008, 281(5): 923-934.

[20] SINGH R K, SENTHILKUMARAN P, SINGH K. Focusing of linearly and circularly polarized Gaussian background vortex beams by a high numerical aperture system afflicted with third-order astigmatism [J]. Optics Communications, 2008, 281(24): 5939-5948.

[21] SINGH R K, SENTHILKUMARAN P, SINGH K. Effect of primary coma on the focusing of a Laguerre-Gaussian beam by a high numerical aperture system; vectorial diffraction theory [J]. Journal of Optics A-Pure and Applied Optics, 2008, 10(075008): 1-9.

[22] DENG S H, LIU L, CHENG Y, et al. Effects of primary aberrations on the fluorescence depletion patterns of STED microscopy[J]. Optics Express, 2010, 18(2): 1657-1666.

[23] DENG S H, LIU L, CHEN Y, et al. Investigation of the influence of the aberration induced by a plane interface on STED microscopy[J]. Optics Express, 2009, 17(3): 1714-1725.

[24] RICHARDS B, WOLF E. Electromagnetic diffraction in optical systems II structure of the image field in an aplanatic system[J]. Proceedings of the Royal Society A, 1959, 253 (1274): 358-379.